Available online at www.sciencedirect.com
SCIENCE DIRECT®
Journal of Sound and Vibration 287 (2005) 989–1003
JOURNAL OF SOUND AND VIBRATION
www.elsevier.com/locate/jsvi

Short Communication

Be careful when using the International Roughness Index as an indicator of road unevenness

Oldřich Kropáč[a], Peter Múčka[b,*]

[a]*Kaňkovského 1241/2, CZ-182 00 Prague 8, Czech Republic*
[b]*Institute of Materials and Machine Mechanics, Slovak Academy of Sciences, Račianska 75, SK-831 02 Bratislava 3, Slovak Republic*

Received 2 April 2004; received in revised form 9 February 2005; accepted 22 February 2005
Available online 26 April 2005

Abstract

Currently, from more road unevenness single-number indicators, the International Roughness Index (IRI) is the most popular. However, some roads with irregular forms of unevenness power spectral density (PSD) require analytical description with a number of independent parameters. In such cases the IRI cannot be used to distinguish between road profiles of distinctly different features. To indicate possible erroneous assessments of road unevenness using the IRI only, a simulation study was conducted in which seven different homogeneous road profiles were considered with waviness values in the range from 1.5 to 3.0, and 0.1—variance component of single harmonic undulation with most dangerous wavelengths, all having the same nominal value IRI = 2.21 mm/m. Values of the comparison single-number indicator, the standard deviation of elevation, were found in the range from 1.48 to 7.065 mm. The effect of selected road profiles on two vehicles, a passenger car and a truck, and on people sitting in the vehicles was also studied yielding even more dissimilar results.

1. Introduction

The vibration of an on-road vehicle is predominantly excited by the unevenness of the road surface on which the vehicle travels. The measured road unevenness is usually considered as a

*Corresponding author. Tel.: +421 02 5930 9420; fax: +421 02 5477 2099.
E-mail addresses: oldrich.kropac@cbox.cz (O. Kropáč), ummsmuc@savba.sk (P. Múčka).

0022-460X/$ - see front matter © 2005 Elsevier Ltd. All rights reserved.
doi:10.1016/j.jsv.2005.02.015

realization $h(l)$ of the random function $H(l)$ where H (m) is the vertical elevation, and l (m) is the distance along the road track. Provided that this function is homogeneous, centred, and Gaussian, its power spectral density (PSD) provides its full statistical description. The PSD $G_H(\Omega)$ of the road unevenness $H(l)$, the so-called (longitudinal) road profile, is usually described by a simple expression [1]

$$G_H(\Omega) = C\Omega^{-w}, \tag{1}$$

where Ω (rad/m) is the circular (angular) spatial frequency, or wavenumber, C $(\text{rad}^{w-1}\,\text{m}^{3-w}) = G_H(1)$ is the unevenness index, and w (1) is the waviness; its value usually ranges from 1.5 to 3, with the typical value $w = 2$.

For practical purposes, especially for the management of road network maintenance management systems, it is often sufficient to work with a single-number indicator of the unevenness level. Currently, the IRI is the most popular one. It is based on a computer program proposed by Sayers [2], which is applied to a particular measured longitudinal profile $h(l)$. In principle, it evaluates the response of a specific 2dof linear vehicle model, the so-called golden car or Reference-Quarter-Car-Simulation (RQCS) travelling at a running speed 80 km/h along the profile. IRI is defined as accumulated suspension stroke (mm) in a reference passenger car divided by travelled distance (m).[1] For $w = 2$, a simple relationship between C (10^{-6} rad m), and IRI (mm/m) holds [3]

$$\text{IRI} = a\sqrt{C}. \tag{2}$$

The value of the coefficient a was established in an extensive simulation study [4] to be $a = 2.21$. In Ref. [4], an expanded relation $\text{IRI} = f(C, w)$ was also determined for w in the range from 1.5 to 3.0 proving that relation (2) likewise holds but with

$$a = 2.21\ \exp(-0.356\Delta w + 0.13(\Delta w)^2), \quad \text{where } \Delta w = w - 2. \tag{3}$$

Real roads, especially of lower surface quality, often exhibit considerably irregular courses of the PSD. Therefore, a further simulation study was undertaken aiming at the effect of unusual forms of the PSD on the above-mentioned unevenness indices C, w, and IRI [5]. Another departure of the PSD of road unevenness from the standard form (1) reflects the presence of additive periodical components in the longitudinal road profile. This effect is quantified in Ref. [6]. For all the studied departures from the standard form considerable changes in the IRI values have been demonstrated. It is evident that the same value of IRI may describe roads with quite different visual features and with differences in other indicators of longitudinal profile.

Therefore, the aim of this paper is to show on particular examples of different road profiles that relying only on IRI may lead to incorrect decisions concerning the real state of the road surface quality.

[1] IRI is a dimensionless quantity of the order 10^{-3}. To avoid repeated citations of this constant, "dimensionless units" (mm/m) or (m/km) (in the U.S also (in/mi)) are currently applied in road management practice.

2. Specifications of comparative road profiles

Based on results of papers [4–6], seven different courses of road profiles were considered (Table 1), all with the same value IRI = 2.21 mm/m corresponding to road unevenness PSD model (1) with $C = 1 \times 10^{-6}$ rad m, $w = 2$ and which may be considered as the basic comparison standard (#2 in further text). It is known from literature, see e.g. Refs. [7–12] that except of practically and analytically preferred value of waviness $w = 2$, many roads exhibit waviness value in a rather wide range from 1.5 to 3.0. Therefore, these limit values 1.5 and 3.0 are considered in profiles #1 and #3, respectively. To obtain the same value of IRI = 2.21 mm/m, recalculation of corresponding C values was done according to formula (2).

In the usually random course of the road profile sometimes periodic components appear the cause of which is discussed, e.g. in Refs. [5,6]. For the sake of simplicity the presence of a single harmonic component was considered in the form

$$H(l) = (1 - q)H_0(l) + qH_1(l), \tag{4}$$

where $H_0(l)$ is the random component of the road profile with the PSD of form (1), and $H_1(l)$ is the harmonic component of the road profile of the form

$$H_1(l) = A_d \cos(2\pi l/l_1), \tag{5}$$

where A_d is the amplitude of the harmonic undulation, and l_1 is its wavelength, and q (1) is the ratio of the variance of the harmonic component D_1 related to the total variance $D_H = D_0 + D_1$.

The partial variances D_0, and D_1 of the components $H_0(l)$, and $H_1(l)$ are expressed as follows [4]

$$D_0 = C(2\pi)^{-w+1}(w - 1)^{-1}(L_M^{w-1} - L_m^{w-1}), \tag{6}$$

where $\langle L_m, L_M \rangle$ is the wavelength range of effectively acting wavelengths of the random road unevenness, L (m) $= 2\pi/\Omega$,

$$D_1 = A_d^2/2. \tag{7}$$

From the above relations, the amplitude A_d of the particular single harmonic component was evaluated as

$$A_d = \sqrt{2D_0 q/(1 - q)}. \tag{8}$$

Table 1
Nominal and mean values of simulated characteristics of road profiles

Profile	C_{nom}/C_{sim} (10^{-6} rad m)	w_{nom}/w_{sim} (1)	q (1)	l_1 (m)	A_d (mm)	IRI_{sim} (mm/m) ($IRI_{nom} = 2.21$)	D_{Hsim1}/D_{Hsim2} (mm^2)	RMS_{Hsim} (mm)	Figures
#1	0.6602/0.6362	1.5/1.5105	0	—		2.1812	3.311/3.259	1.805	1
#2	1/0.9384	2/1.9987	0	—		2.1907	8.527/7.834	2.799	2
#3	1.5767/1.6028	3/3.0381	0	—		2.2484	66.268/49.911	7.065	3
#4	0.2516/0.2648	2/2.0180	0.1	2.21	0.6610	2.2198	2.344/2.189	1.479	4a, 4b, 4c
#5	0.8564/0.9527	2/2.1020	0.1	6.25	1.2274	2.2120	8.389/7.462	2.732	5a, 5b, 5c
#6	0.7843/0.9771	3/3.1783	0.1	6.25	2.3489	2.2221	35.947/27.586	5.252	6a, 6b, 6c
#7	—/0.0013	—/6.6759	1	6.25	3.0123	2.2083	4.5366/4.5370	2.13	7a, 7b, 7c

For simulation, a value $q = 0.1$ was found as adequately describing situations on real roads. In Refs. [5,6], the wavelengths of the harmonic component $l_1 = 2.21$, and 6.25 m were estimated to be critical for both passenger cars and trucks travelling at the running speed 90 km/h. The wavelength near 2.21 m may appear, e.g. ahead of road crossings controlled by traffic lights where the periodic undulation is probably due to the braking of vehicles. The wavelength near 6.25 m corresponds to rigid (concrete) pavement with defectively sealed expansion joints between slabs, or to provisional pre-cast slab concrete pavements. Thus, the wavelength $l_1 = 2.21$ m was used in the road profile #4 and the wavelength $l_1 = 6.25$ m in the road profiles #5 and #6. As for profile #7, a single harmonic undulation (i.e. $q = 1$) with wavelength $l_1 = 6.25$ m was used as a limiting comparative example.

3. Standard deviations of the vertical road elevation

For each of the above-defined longitudinal profiles (with the exception of #7) ten replicated independent realizations were generated using a sum of harmonic functions with wavelengths within the range from 0.3 to 90 m with random phase uniformly distributed over the interval $(0, 2\pi)$. For road profiles generation according to prescribed PSDs the procedure given in Ref. [13] was used. The total length of all profiles was 819.2 m with sampling interval of 0.1 m. The relevant quantities were estimated from the $\mathrm{PSD}_{\mathrm{sim}}$ in the wavelength range $\langle 0.78\,\mathrm{m}, 50\,\mathrm{m} \rangle$. The same wavelength range was used when evaluating extensive results of the WRA-EVEN experiment [14] aimed at comparison and possible unification of very different methodological approaches, measuring devices, introduced characteristics, and consequent estimation procedures for road surface quality assessment. This wavelength range is also included in a pertinent European standard being currently in preparation stage [15]. For estimation of C_{sim}, w_{sim} the procedure given in Ref. [15], Appendix C, was used. All the computations were made in Matlab. The nominal and simulated mean values of those quantities are summarized in Table 1, where in addition, the total variance $D_{H\mathrm{sim}}$ is given too. Two estimates of $D_{H\mathrm{sim}}$ are given, one obtained by integration of $\mathrm{PSD}_{\mathrm{sim}}$—data with subscript 1—the other one by analytical evaluation—subscript 2. Due to local irregularities of the $\mathrm{PSD}_{\mathrm{sim}}$, $D_{H\mathrm{sim1}} > D_{H\mathrm{sim2}}$ must hold. Note the rather large differences between both estimates for cases #3 and #6, both for profiles with waviness $w = 3$. Note also that presence of harmonic undulation slightly decreases the values of the variance D_H. The difference between cases #4 and #5, which have the same parameters, with the exception of l_1, is due to the different gain of the IRI algorithm in relation to the wavelengths. For $l_1 = 2.21$ m, it takes one of the local maximum value ≈ 1.6, while for $l_1 = 6.25$ m, it takes the local minimum value ≈ 1.13. For the pure harmonic undulation—case #7, C_{sim} and w_{sim} have no practical sense, since they only reflect the numerical noise of the computing algorithm used. It seems useful to use the standard deviation of elevation $\mathrm{RMS}_H = \sqrt{D_{H\mathrm{sim2}}}$ as an alternative single-number indicator of road longitudinal unevenness. The particular values of RMS_H are also given in Table 1. In order to illustrate the visual feature of simulated profiles, their courses are depicted in Figs. 1–3, and 4a–7a. For cases #4–#7, also their PSDs and correlation functions $\rho(\lambda)$ (CFs) are shown in Figs. 4b–7b, and 4c–7c, respectively. Again, Fig. 7b reflects the numerical noise only of the applied computing algorithm.

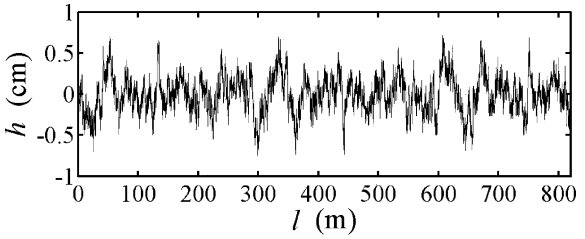

Fig. 1. Sample realization of the road profile #1.

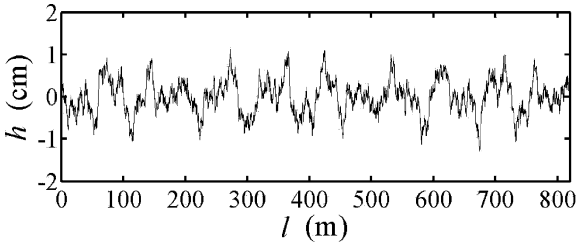

Fig. 2. Sample realization of the road profile #2.

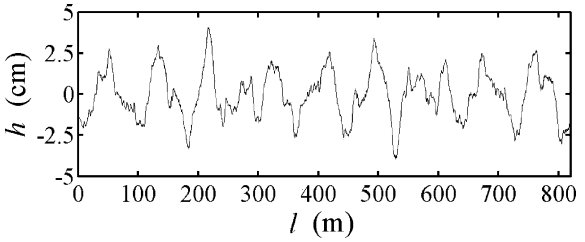

Fig. 3. Sample realization of the road profile #3.

4. Effect of unevenness on the response of travelling vehicles

Inspection of Figs. 1–7a, and data in Table 1, especially those in the column $\mathrm{RMS}_{H\mathrm{sim}}$, enables to state that for the same IRI value, quite different values of alternative indicators of road unevenness may be observed. Particularly, when considering the $\mathrm{RMS}_{H\mathrm{sim}}$, the variability spans from 1.48 to 7.06 mm with the "normal" value 2.8 mm corresponding to the standard profile #2. To indicate the influence of various profiles on travelling vehicles two cases are considered.

First, we observe the planar 12-dof model of a typical passenger car occupied by a driver and a passenger. The particular form and parameters of this case are published in Refs. [6,16], and for a reader's convenience reproduced in Fig. 8a. As quantities of practical interest, driver's and passenger's vertical accelerations were analysed at the seat–driver interface, i.e. masses m_{3d}, m_{3p} (used for comfort assessment) and at their heads, i.e. masses m_{6d}, m_{6p} (receptivity of the surroundings influencing driving safety). At the seat–driver/passenger interfaces, the frequency

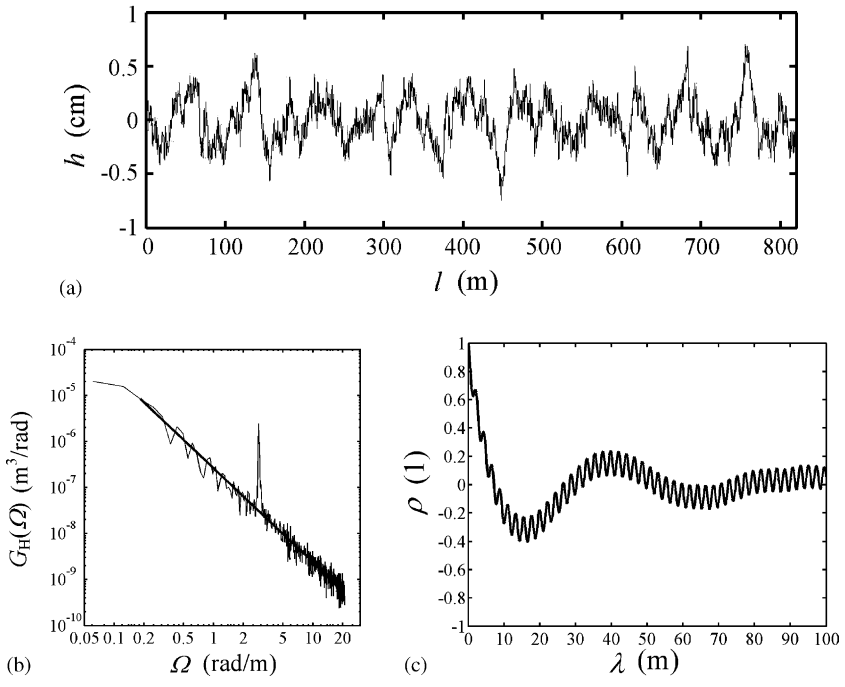

Fig. 4. Characteristics of the road profile #4: (a) sample realization, (b) PSD, (c) CF.

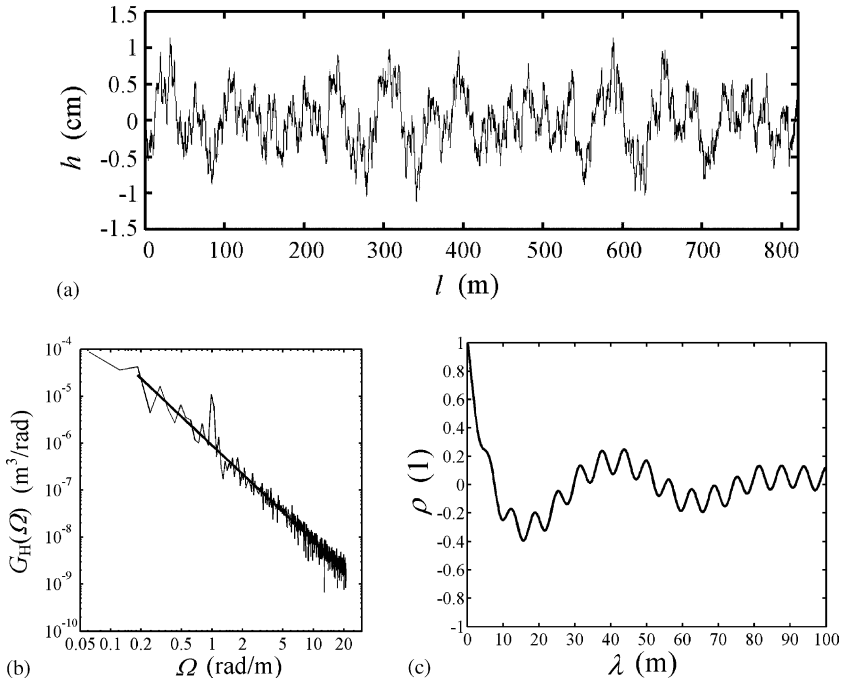

Fig. 5. Characteristics of the road profile #5: (a) sample realization, (b) PSD, (c) CF.

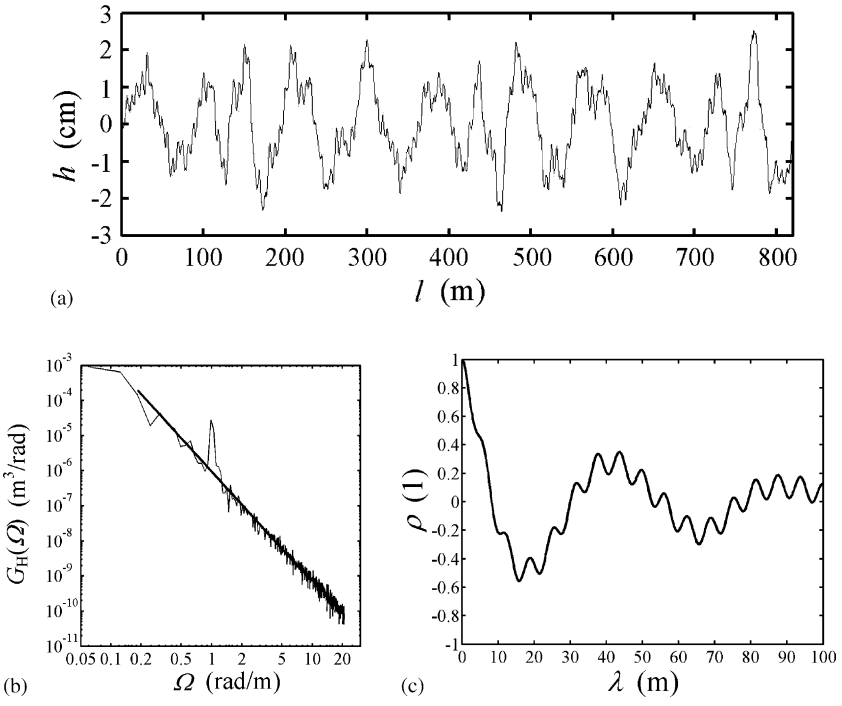

Fig. 6. Characteristics of the road profile #6: (a) sample realization, (b) PSD, (c) CF.

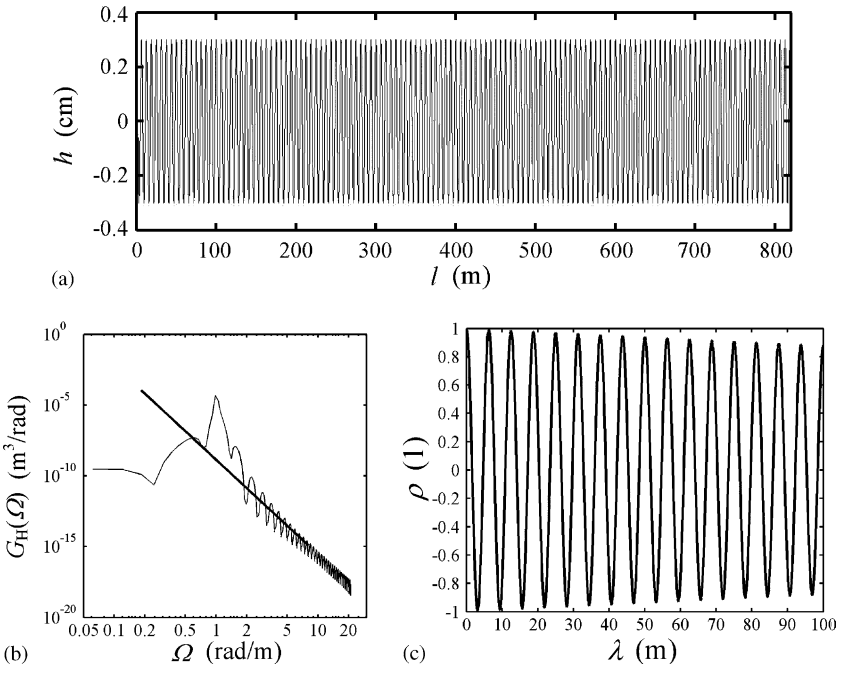

Fig. 7. Characteristics of the road profile #7: (a) sample realization, (b) PSD, (c) CF.

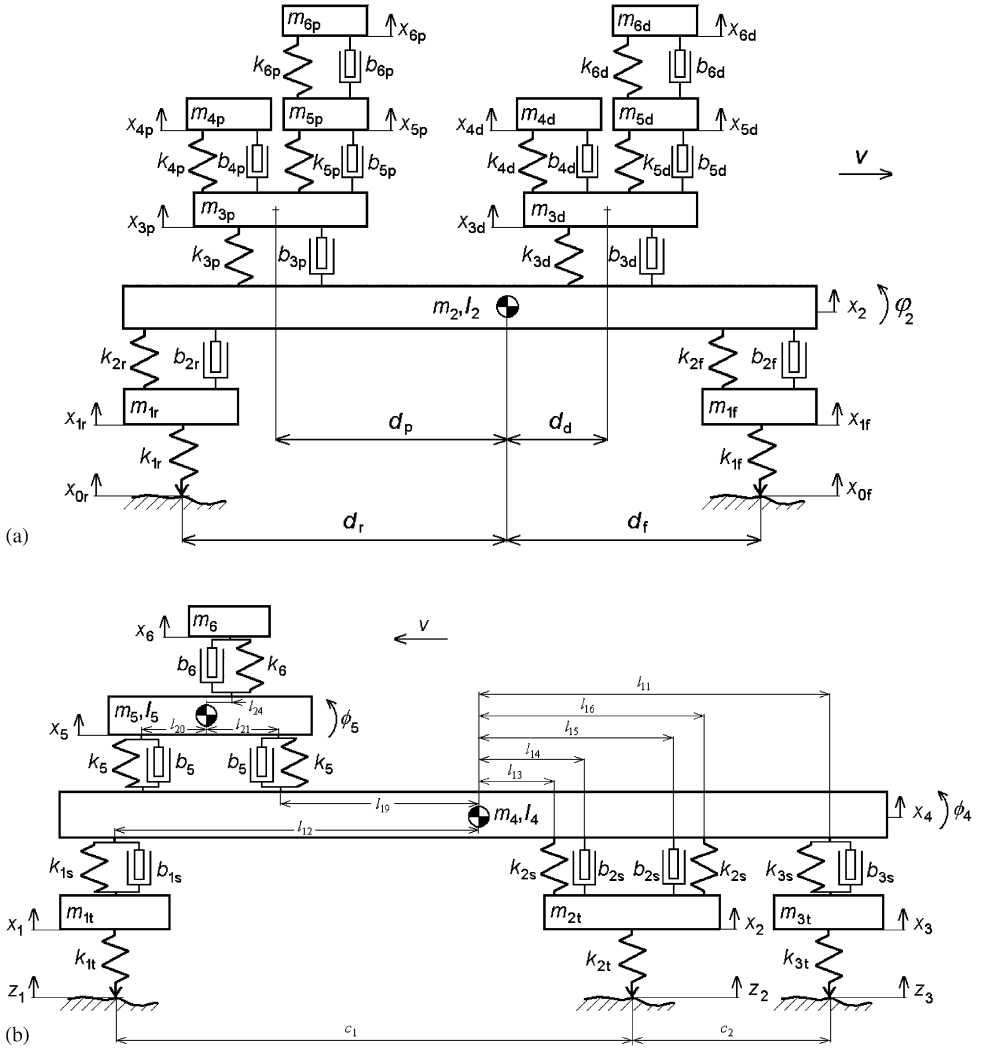

Fig. 8. (a) The planar model of a passenger car, (b) the planar model of a three-axle truck.

weighting according to ISO 2631-1 [17] was taken into account which reduces to some extent the effective values of acceleration relevant for travel comfort assessment. Also, the tyre forces acting on front and rear axles were calculated. The statistical evaluation of data concerning acceleration is presented in Fig. 9, that concerning the dynamic load coefficient $\mathrm{DLC} = (\mathrm{RMS}\, F_d)/F_{\mathrm{stat}}$ in Fig. 10. Mean values of all values simulated on this car are presented in the Appendix, Table 2. Selected quantities of accelerations are also plotted in Fig. 11, values of the DLC are visualized in Fig. 13.

Second, the 8-dof planar model of a three-axle truck of medium carrying capacity is depicted in Fig. 8b. The detailed description and parameters used were published in Refs. [6,18]. Evaluated

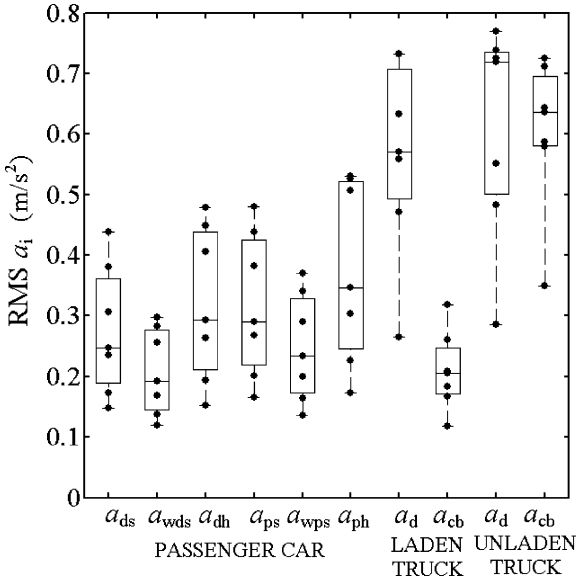

Fig. 9. The RMS values of accelerations for the passenger car and the truck for profiles #1–#7: ranges, mean values, quartiles (rectangles); subscripts: ds—driver's seat, wds—weighted driver's seat, dh—driver's head, ps—passenger's seat, wps—weighted passenger's seat, ph—passenger's head, d—driver, cb—car-body.

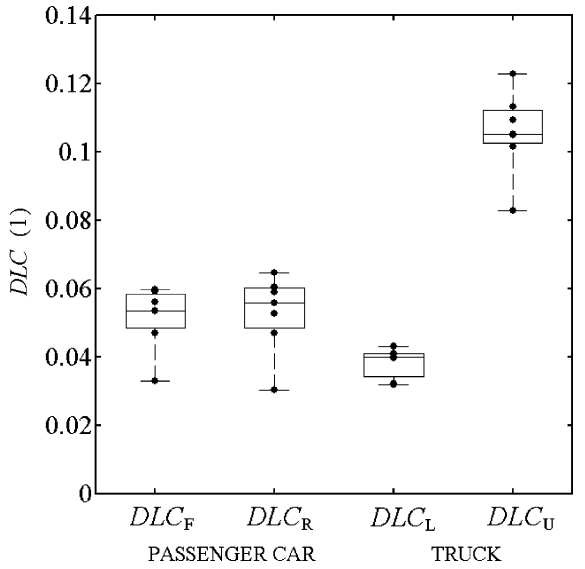

Fig. 10. The values of the dynamic load coefficient (DLC) for profiles #1–#7: ranges, mean values, quartiles (rectangles); subscripts: F—passenger car front axle, R—passenger car rear axle, L—laden truck, U—unladen truck.

accelerations of car-body a_{cb} (C.G. of mass m_4 in Fig. 8b) and driver a_d (mass m_6 in Fig. 8b) are visualized in Fig. 12, and DLCs relevant for the driven (middle) axle are shown in Fig. 13. Mean values of all data simulated on this truck are reproduced in the Appendix, Table 3.

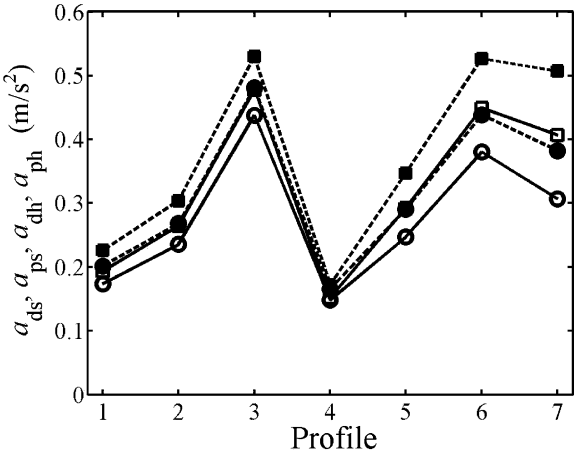

Fig. 11. The RMS values of selected vertical accelerations of the passenger car for profiles #1–#7: driver's head (-□-); driver's seat (-○-); passenger's head (-■-); passenger's seat (-●-).

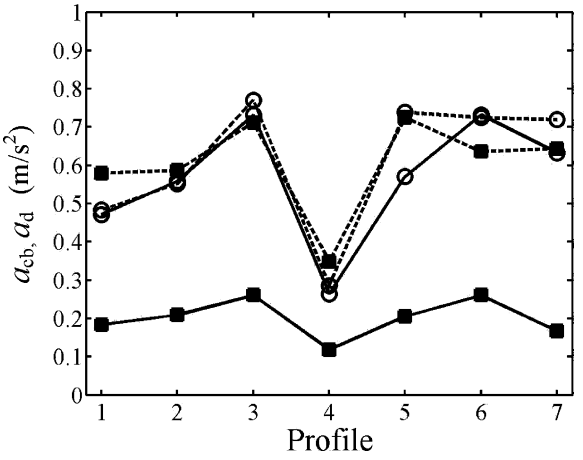

Fig. 12. The RMS values of the vertical accelerations of the truck for profiles #1–#7: car-body, laden truck (-■-); car-body, unladen truck (–■–); driver, laden truck (-○-); driver, unladen truck (–○–).

Rather large variability in accelerations can be observed on people sitting in the vehicles. Therefore, in Fig. 14, selected values of accelerations are plotted in relation to $\mathrm{RMS}_{H\mathrm{sim}}$, ordered according to their actual values. When data for profiles #5 and #7 are omitted, the remaining relations are approximately situated on a "smooth" line. This can be interpreted in such a way that RMS_H could be considered as an alternative single-parameter indicator of road unevenness for rather different types of unevenness. Nevertheless, it must be noted that the RMS_H strongly depends on L_M^{w-1} (see Eq. (6)), where the proper estimation of the maximal effectively acting

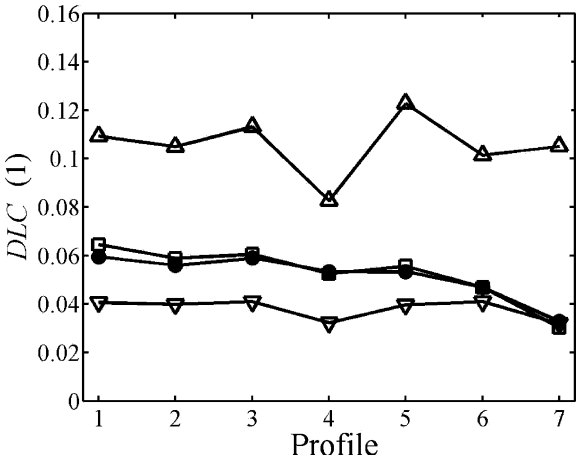

Fig. 13. The values of the dynamic load coefficient (DLC) for profiles #1–#7: passenger car front wheel (-●-); passenger car rear wheel (-□-); laden truck (-▽-); unladen truck (-△-).

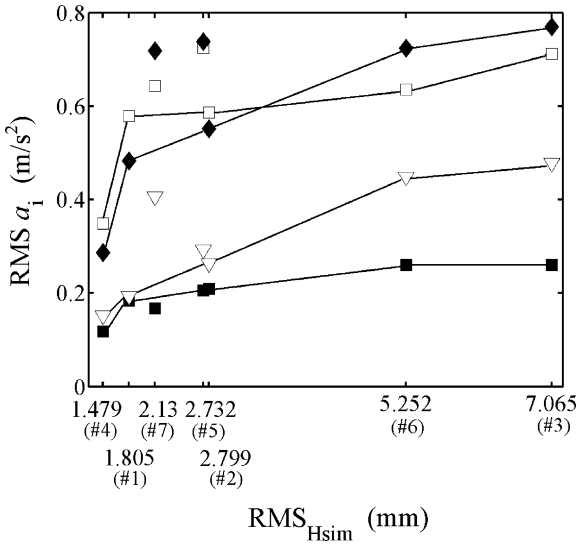

Fig. 14. The RMS values of selected accelerations as functions of rms elevation, RMS$_H$: car-body, laden truck (-■-); car-body, unladen truck (-□-); driver, unladen truck (-◆-); driver's head, passenger car (-▽-).

unevenness wavelength L_M (which depends on the design speed of the particular road, see e.g. Ref. [4]) might be a critical task. Points for cases #5 and #7 belong to cases with periodical components with the wavelength $l_1 = 6.25$ m (although the corresponding RMS$_H$ is rather low) what indicates the increased severity of this type of unevenness especially for the stressing of the driver of a truck.

5. Conclusions

In this paper, simplified analytical models of road unevenness were applied, nevertheless, they cover rather wide variety of examples appearing in the traffic practice, so that the presented results provide a brief insight into the problem in question. For the comparison model #2, value of C was chosen at 1×10^{-6} rad m, which corresponds to the geometric mean of the best road surface quality class according to Ref. [1]. Therefore, the running speed 90 km/h was found appropriate for simulation.

From the data and figures presented in this paper, following main conclusions can be drawn.

(1) The same value of IRI may be obtained for a variety of road profiles which considerably differ both in the subjectively judged visual features, as well as in generally accepted physically and/or analytically based unevenness indicators. The ratio of the largest and lowest RMS values of the road elevation for parameters considered in this study is 4.77.

(2) Considering the response of the vehicle to the road unevenness, which is of even greater practical interest than the level of unevenness itself, it was shown that the most expressive effect of the unevenness displays on people travelling in the vehicle. The ratio of max/min values of head vertical acceleration is 3.53 for the passenger's head in the passenger car, and 2.77 for the driver for a laden, and 2.69 for an unladen truck. For absolute range of acceleration values this means a reduction of allowable exposure to vibration for people in the vehicle even by some hours. On the other hand, the change of the effect on the freight (cargo) of the laden truck is not so marked with the max/min ratio 2.2. The least variability was observed for the DLC, whose max/min values are 1.78, and 1.94 for front and rear axles of the passenger car, respectively, and 1.29 and 1.48 for a laden and an unladen truck, respectively.

(3) Among profiles considered in this simulation study, those with the waviness values $w = 3$ (cases #3, #6) display the highest RMS_H and consequently, highest values of all observed accelerations. Random unevenness with the waviness value $w = 3$ appears predominantly at high-quality pavements (low C) of high-speed motorways and airport runways. Just for this waviness, the IRI indicator *underestimates* the road unevenness state by a factor of the order of 0.8.

(4) Surprisingly, the presence of low-percentage single harmonic component ($q = 0.1$) decreases the unevenness RMS_H but the acceleration response remarkably increases in comparison to the pure random course. This analogically applies for the pure harmonic undulation ($q = 1$).

For comparison, the standard deviation of vertical elevation RMS_H was proposed as an alternative single-number indicator to the IRI. From the presented study, it seems that this indicator has some advantages in comparison to the commonly used indicator IRI. This is probably the reason that, reflecting the different importance of short, medium, and long road unevenness on the vehicle vibration, the use of three RMS_H values (or corresponding variances D_H) for short, medium, and long partial intervals of the whole effectively acting wavelength band for more detailed characterization of the road unevenness [5] gained recently popularity in some European countries.

To sum up, the warning given in the title of this paper seems to be fully justifiable.

Appendix

The RMS values of response on passenger car and on truck are given in Tables 2 and 3.

Table 2
The RMS values of the response on passenger car for $v = 90$ km/h

Profile	Driver's seat acceleration	Driver's weighted seat acceleration	Driver's head acceleration	Passenger's seat acceleration	Passenger's weighted seat acceleration	Passenger's head acceleration	Front wheel dynamic tyre force	DLC front wheel	Rear wheel dynamic tyre force	DLC rear wheel
	a_{ds} (m/s^2)	a_{wds} (m/s^2)	a_{dh} (m/s^2)	a_{ps} (m/s^2)	a_{wps} (m/s^2)	a_{ph} (m/s^2)	F_{df} (kN)	DLC_F (1)	F_{dr} (kN)	DLC_R (1)
#1	0.1735	0.1369	0.1934	0.2017	0.1638	0.2257	0.3567	0.0595	0.3353	0.0645
#2	0.2355	0.1682	0.2641	0.2684	0.2001	0.3039	0.3356	0.0559	0.3062	0.0589
#3	0.4379	0.2559	0.4781	0.4807	0.2903	0.5299	0.3543	0.0590	0.3147	0.0605
#4	0.1481	0.1190	0.1519	0.1656	0.1351	0.1724	0.3207	0.0534	0.2733	0.0526
#5	0.2475	0.1923	0.2925	0.2902	0.2339	0.3472	0.3197	0.0533	0.2899	0.0557
#6	0.3804	0.2830	0.4493	0.4388	0.3411	0.5268	0.2812	0.0469	0.2441	0.0469
#7	0.3066	0.2970	0.4066	0.3823	0.3708	0.5072	0.1966	0.0328	0.1576	0.0303
Mean	0.2756	0.2075	0.3194	0.3182	0.2479	0.3733	0.3093	0.0515	0.2744	0.0528
STD	0.1060	0.0715	0.1274	0.1192	0.0893	0.1493	0.0558	0.0093	0.0594	0.0114

Table 3
The RMS values of the response on truck for $v = 90$ km/h (laden/unladen)

Profile	Driver's acceleration	Car body acceleration	Driven axle wheel dynamic tyre force	Dynamic load coefficient
	a_{dL}/a_{dU} (m/s^2)	a_{cbL}/a_{cbU} (m/s^2)	F_{d2L}/F_{d2U} (kN)	DLC_L/DLC_U (1)
Laden/unladen				
#1	0.4718/0.4833	0.1836/0.5795	2.4219/2.5030	0.0407/0.1093
#2	0.5583/0.5513	0.2090/0.5870	2.3767/2.4026	0.0399/0.1049
#3	0.7331/0.7702	0.3183/0.7120	2.5547/2.5889	0.0429/0.1131
#4	0.2645/0.2861	0.1183/0.3489	1.9142/1.8923	0.0322/0.0826
#5	0.5708/0.7383	0.2053/0.7250	2.3619/2.8100	0.0397/0.1227
#6	0.7322/0.7245	0.2607/0.6360	2.4398/2.3242	0.0410/0.1015
#7	0.6325/0.7192	0.1671/0.6437	1.8979/2.4066	0.0319/0.1051
Mean	0.5662/0.6104	0.2089/0.6046	2.2810/2.4182	0.0383/0.1056
STD	0.1632/0.1787	0.0649/0.1257	0.2636/0.2815	0.0044/0.0123

Recently, a relevant paper [19] of the authors appeared in which it has been demonstrated that applying the IRI algorithm the road waviness can be estimated from the longitudinal road profile.

References

[1] International Organization for Standardization ISO 8608, Mechanical vibration—Road surface profiles—Reporting of measured data, 1995.
[2] M.W. Sayers, On the calculation of IRI from longitudinal road profile, Transport Research Board, Washington, DC, Paper No. 950842, 1995, 24pp.
[3] O. Kropáč, Characteristics of longitudinal road unevenness: definition, estimation and use, *Strojnícky časopis* 52 (2001) 325–359.
[4] O. Kropáč, P. Múčka, Relations between characteristics of longitudinal unevenness of roads: a review, *Strojnícky časopis* 54 (2003) 49–64 (Erratum and amendments, ibid., 188–194).
[5] O. Kropáč, P. Múčka, Non-standard longitudinal profiles of roads and indicators for their characterization, *International Journal of Vehicle Design* 36 (2004) 149–172.
[6] O. Kropáč, P. Múčka, Longitudinal road unevenness with periodic components: characterization and effects on people in traversing vehicle, Proceedings of Institution of Mechanical Engineers, Part D, *Journal of automobile Engineering*, in press.
[7] H. Braun, Untersuchungen über Fahrbahnunebenheiten, Deutsche Kraftfahrtforschung und Strassenverkehrstechnik, VDI-Berichte Nr. 186, VDI-Verlag, Düsseldorf, 1966.
[8] R.S. Sayles, T.R. Thomas, Surface topography as a non-stationary random process, *Nature* 271 (1978) 431–434 (Comments by M.V. Berry, J.H. Hannay with authors' replay, ibid., 573).
[9] H. Braun, Messergebnisse von Strassenunebenheiten, VDI-Berichte Nr. 877, VDI-Verlag, Düsseldorf, 1991.
[10] J. Šprinc, O. Kropáč, M. Šprinc, Characterization of longitudinal road unevenness in the light of the International PIARC-EVEN experiment 1998, *Vehicle System Dynamics* 37 (2002) 263–281.
[11] P. Múčka, The road waviness and the dynamic tyre force, *International Journal of Vehicle Design* 36 (2004) 216–232.
[12] M. Decký, Evaluation of Longitudinal Unevenness by a Double-mass Measuring Set JP VSDS, PhD Thesis, University of Žilina, 1996.

[13] J. Čačko, M. Bíly, J. Bukoveczky, *Random Processes: Measurement, Analysis, and Simulation*, Elsevier, Amsterdam, 1988.
[14] D.-M. Ducros, L. Petkovic, G. Descornet, B. Berlémont, M. Alonso Anchuelo, S. Yanguas, W. Jendryka, P. Andrén, FILTER experiment—longitudinal analyses, FEHRL Final Report 2001/1, Paris, Laboratoire Central des Ponts et Chaussées.
[15] prEN 13036-5, Road and airfield characteristics, determination of longitudinal unevenness indices, CEN/TC 227/WG 5/TG 1, draft 3.1 on 18 October 2002.
[16] G.J. Stein, P. Múčka, Theoretical investigation of a planar model of a personal car with seated people, *Proceedings of Institution of Mechanical Engineers, Part D, Journal of Automobile Engineering* 217 (2003) 257–268.
[17] International Organization for Standardization ISO 2631-1, Mechanical evaluation of mechanical vibration and shock—evaluation of human exposure to whole body vibration—part 1: general requirements, 1997.
[18] P. Múčka, The active suspension of heavy vehicle driven axle, *Strojnícky časopis* 53 (2002) 153–165 (in Slovak).
[19] O. Kropáč, P. Múčka, Estimation of road waviness using the IRI algorithm, *Strojnícky časopis* 55 (2004) 308–313.